Journal of Structural Biology 185 (2014) 125–128

Contents lists available at ScienceDirect

Journal of Structural Biology

journal homepage: www.elsevier.com/locate/yjsbi

Technical Note

A new tool based on two micromanipulators facilitates the handling of ultrathin cryosection ribbons ☆

Daniel Studer [a], Alycia Klein [a], Ioan Iacovache [a], Helmut Gnaegi [b], Benoît Zuber [a,*]

[a] Laboratory of Experimental Morphology, Institute of Anatomy, University of Bern, Baltzerstrasse 2, 3000 Bern 9, Switzerland
[b] Diatome SA, Helmstrasse 1, 2560 Nidau, Switzerland

ARTICLE INFO

Article history:
Received 22 August 2013
Received in revised form 13 November 2013
Accepted 16 November 2013
Available online 21 November 2013

Keywords:
Cryosectioning
Frozen-hydrated sections
Ultramicrotomy
Electron microscopy
High pressure freezing
Cryo-electron microscopy
Micromanipulation

ABSTRACT

A close to native structure of bulk biological specimens can be imaged by cryo-electron microscopy of vitreous sections (CEMOVIS). In some cases structural information can be combined with X-ray data leading to atomic resolution in situ. However, CEMOVIS is not routinely used. The two critical steps consist of producing a frozen section ribbon of a few millimeters in length and transferring the ribbon onto an electron microscopy grid. During these steps, the first sections of the ribbon are wrapped around an eyelash (unwrapping is frequent). When a ribbon is sufficiently attached to the eyelash, the operator must guide the nascent ribbon. Steady hands are required. Shaking or overstretching may break the ribbon. In turn, the ribbon immediately wraps around itself or flies away and thereby becomes unusable. Micromanipulators for eyelashes and grids as well as ionizers to attach section ribbons to grids were proposed. The rate of successful ribbon collection, however, remained low for most operators. Here we present a setup composed of two micromanipulators. One of the micromanipulators guides an electrically conductive fiber to which the ribbon sticks with unprecedented efficiency in comparison to a not conductive eyelash. The second micromanipulator positions the grid beneath the newly formed section ribbon and with the help of an ionizer the ribbon is attached to the grid. Although manipulations are greatly facilitated, sectioning artifacts remain but the likelihood to investigate high quality sections is significantly increased due to the large number of sections that can be produced with the reported tool.

1. Introduction

Biological structures close to their native state are best resolved in cryo-electron microscopy. Very thin samples (less than 1 μm in thickness) are directly investigated after plunge freezing. Bulk samples are investigated by CEMOVIS (Cryo-Electron Microscopy Of Vitreous Sections). With both approaches the structures are fully hydrated and depicted by phase contrast. No staining is necessary and therefore the real structure is depicted, in contrary to all other thin-sectioning electron microscopy (EM) techniques that actually reveal an affinity map for heavy metal stains (for review see Hurbain and Sachse, 2011).

First attempts to produce cryosections were published by Fernandez-Moran and Dahl, (1952) and many others, but water was crystalline and for about 20 years the sections were dried before EM observation, which both lead to severe artifacts. Pioneers of CEMOVIS are Hutchinson, Zierold, Frederik, McDowall (references in the review by Dubochet et al., 1988). High pressure freezing made it possible later on to vitrify many bulk samples (for review see Studer et al., 2008). This may be the main reason why the number of high-resolution CEMOVIS studies has significantly increased in the last 10 years (Al-Amoudi et al., 2007; Al-Amoudi et al., 2011; Couture-Tosi et al., 2010; Eltsov et al., 2008; Hoog et al., 2012; Leforestier et al., 2012; Matias et al., 2003; Pierson et al., 2011; Saibil et al., 2012; Salje et al., 2009; Scheffer et al., 2011; Zuber et al., 2005, 2008). Nonetheless the number of CEMOVIS reports remained quite low in comparison to publications on plunge-frozen samples, because CEMOVIS has been technically demanding. Furthermore sectioning of vitreous samples is associated with a number of artifacts, such as compression, knife marks, crevasses, chattering and creasing. Most of them can be minimized; however, to date they cannot be completely eliminated (Al-Amoudi et al., 2005; Han et al., 2008). The sectioning process depends too much on the momentary conditions near the cutting edge of the knife in the cryochamber (humidity, charging, section thickness, sample properties, etc.). These problems still await a solution. Based on our long-standing experience we learned that in a ribbon some sections show very pronounced artifacts, some less pronounced ones and sometimes a section is almost free of artifacts. Even within a single section one area can be almost perfect whereas another

* Corresponding author.
E-mail address: zuber@ana.unibe.ch (B. Zuber).

1047-8477/$ - see front matter © 2013 The Authors. Published by Elsevier Inc. All rights reserved.
http://dx.doi.org/10.1016/j.jsb.2013.11.005

area shows stronger artifacts. Because a perfect section is rarely produced, the number of CEMOVIS users has remained relatively modest.

The protocol for cryosectioning and some associated pitfalls were outlined in the abstract. Attempts to improve cryosectioning by the use of micromanipulators were made by others. A micromanipulator to facilitate ribbon guiding with an eyelash was introduced (Ladinsky et al., 2006). However, this manipulation is still being performed by hand in many laboratories. On the other hand, electron microscopic grids can be manipulated by another micromanipulator (Leica Microsystems, Vienna, Austria). The combination of both was so far not reported. The last step of cryosectioning is the firm attachment of the ribbons to the grid by electrostatic charging (Pierson et al., 2010).

Our new setup consists of two micromanipulators. Critically, the ribbon shows unprecedented adhesion to the conductive fiber guided by the manipulator. The setup significantly facilitates the production of section ribbons of vitreous samples. This helps to collect a large number of sections, and therefore the probability to have good ones among them is strongly increased. This will hopefully contribute to raising the usage of CEMOVIS.

2. Sample preparation

As stated above, cryosections show a number of artifacts. To minimize them, the following measures have to be taken. The first condition is that the bulk sample has to be vitreous (no ice crystals in the sample). High pressure freezing is used in most cases for vitrification of bulk samples (Michel et al., 1991; Studer et al., 1995). For the cryosectioning tests presented here, yeast cells (*Saccharomyces cerevisiae*, paste from local grocery store) were high pressure frozen. The yeast paste was resuspended in distilled water for 2 h. The suspension was centrifuged and the supernatant discarded. The pellet was mixed 1:1 with a 20% (w/w) aqueous dextran solution (70 kDa; Sigma–Aldrich, product number: 31390). This mixture was inserted into copper tubes as described earlier (Studer et al., 2001) and used for high pressure freezing in an EM PACT2 (Leica Microsystems). This procedure leads to vitreous samples (cells and solution are vitreous). Any other vitreous sample that can be mounted and trimmed in the ultramicrotome would fulfill the requirements for our tests.

3. Start of cryosectioning

Cryo-ultramicrotomy is performed in a cryochamber mounted on an ultramicrotome. We used a Leica EM UC6 ultramicrotome with an EM FC6 cryochamber (Leica Microsystems; UC7 and FC7 were used as well). The copper tube containing the vitreous sample is mounted on the appropriate chuck of the cryo-microtome at a temperature of −150 °C (this temperature is maintained for all subsequent manipulations). Then the sample is trimmed. A well-trimmed sample is the second condition to get good cryosections. The tip (whole diameter) of the copper rod is cut away with the help of a trimming diamond (45° Diatome, Nidau, Switzerland). The feed is set to 200 nm and the speed at maximum (100 mm/s). Trimming of the whole copper tube can be stopped when the entire surface of the sample in the tube appears evenly black. In most cases such a sample is vitreous. The second step is trimming of a pyramid using the same sectioning parameters as before. The top square of the pyramid has a length of about 100 μm. The height of the pyramid is approximately 30 μm. With such a pyramid cryosectioning is started.

The third condition to get good sections is the use of an ionizer (EM Crion, Leica Microsystems) and the last condition is a good diamond knife (35° diamond knife, Diatome). During sectioning the ionizer is used in the so-called discharge mode in order to reduce electrostatic charging and facilitate section gliding. The feed is set to 50 nm, the ionizer is set to maximum power, and the sectioning speed is set to 1 mm/s for producing a primary ribbon (3–6 sections). If the cryo-microtome is left to work under the set conditions, the primary ribbon bends by itself over the diamond surface during the sectioning process.

4. Micromanipulators

Here we introduce two micromanipulators (Fig. 1) that greatly facilitate ribbon handling. The micromanipulators are manually driven along three perpendicular axes by micrometers. One micromanipulator guides the ribbon by means of an electrically conductive and grounded fiber and it is operated by the user's left hand; the other one guides a grid and is operated with the right hand. The latter micromanipulator can be swung away, which enables the operator to introduce an eyelash fixed on a wooden stick as usually applied in cryo-ultramicrotomy. This is an important feature for manually removing debris when trimming the sample, or to remove and guide ribbons in special cases. The use of an electrically conductive fiber to guide the ribbon is a novel and key feature. This fiber can irreversibly bind the primary ribbon, which

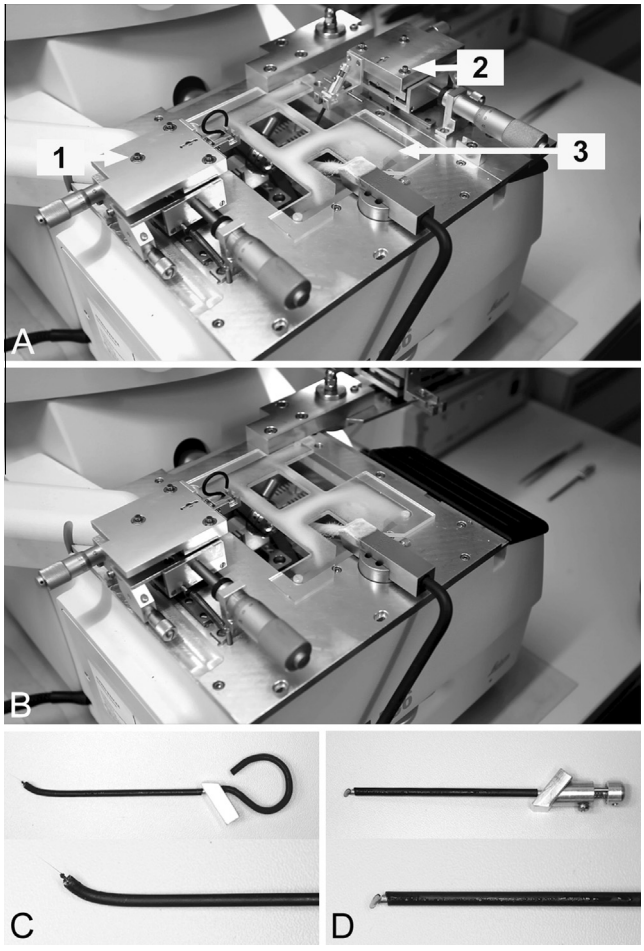

Fig.1. Micromanipulator system. In (A) and (B) the two micromanipulators mounted on top of the cryochamber are depicted. The left one (1) is permanently fixed and drives the conducting fiber depicted in (C). The right micromanipulator (2) holds the EM grid (shown in (D)). It is only used during the transfer of the ribbon onto the grid (A). The rest of the time, it is swung away (as shown in (B)) to give the operator better access to the cryochamber. Label (3) shows the plastic cover designed to minimize ice contamination.

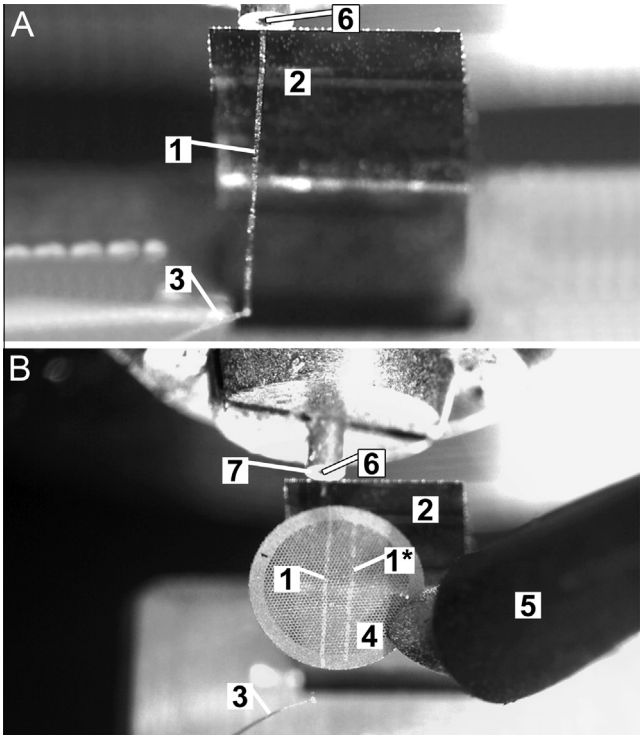

Fig.2. In (A) a section ribbon (1) is shown during its growth. The ribbon is attached to the diamond knife (2) and to the conductive fiber (3). When sectioning is stopped at this stage the ribbon remains stable for hours. In (B) a grid (4) is positioned and the ribbon (1) is attached to it. Note that in this case, another ribbon (1*) was already present on the grid. The grid is clamped by the grid holder (5). The sample (6) was high pressure frozen in a copper tube (7).

greatly facilitates ribbon handling. The fiber consists of a metal-coated guinea pig hair. It is connected to a metallic rod (Fig. 1C) that can be easily clipped onto the micromanipulator. The following steps are shown in Supplementary Movie 1. First, as mentioned above, a ribbon of 3–6 sections is produced without guiding it. At this length, the ribbon curls on the surface of the diamond. Sectioning and ionizer are stopped. The conductive fiber is positioned beneath the primary ribbon with the help of the micromanipulator. To attach the ribbon to the fiber, an ionizer stroke in charge mode was applied. This mode was originally developed to electrostatically attach sections on EM grids (Pierson et al., 2010). Once the ribbon is fixed to the fiber, the ionizer is set to discharge mode, and sectioning is restarted. After each cut, the micromanipulator is driven away from the knife edge with one of the micrometers in order to keep the ribbon under moderate tension (the ribbon should be stretched between the knife edge and the fiber; no bending should be allowed). It is important that the ionizer is positioned close enough and set to a strong enough power to provide sufficient section gliding. However, if the applied ionizer power is too high, the ribbon will start to vibrate strongly, which may lead to ribbon breaking. In this case ionizer power should be gradually reduced until moderate or no vibration occurs. (*Note:* The efficiency of the ionizer very much depends on minimizing grounded material in the vicinity of its tip. This is the main reason why the second micromanipulator is not introduced in the cryochamber before it is used.) In this way ribbons can be produced as long as a few centimeters. However in practice, a ribbon slightly longer than 3 mm (~30 sections) is sufficient. Once this is achieved, sectioning and ionizer are stopped. The second micromanipulator is swung in and locked in operating position (Fig. 1A). The grid holder, to which a grid has previously been mounted, is clipped to the second micromanipulator (Fig. 1D). The mounting is done in such a way that the grid side facing the knife edge is somewhat higher than the opposite side. The grid edge can thus be approached up to a distance of a few tens of micrometers from the knife edge below the ribbon. Subsequently, the fiber is lowered to bring the whole ribbon very close to the grid surface. Care should be taken not to overstretch the ribbon during this procedure. Therefore it might be necessary to move the fiber slightly closer to the knife edge to release tension before lowering it towards the grid. An ionization stroke (charge mode) is then applied and firmly attaches the ribbon to the grid (Fig. 2). The grid is moved with the micromanipulator away from the knife until it is safe to unclip the grid holder from the micromanipulator. The grid is then released into a grid box; a mechanism similar to a mechanical pencil allows easy manipulation.

Attempts to motorize the micromanipulators were unsatisfactory. In our hands, the control of fiber motion is much better by operating micrometers manually. Guiding of the growing ribbon is easier.

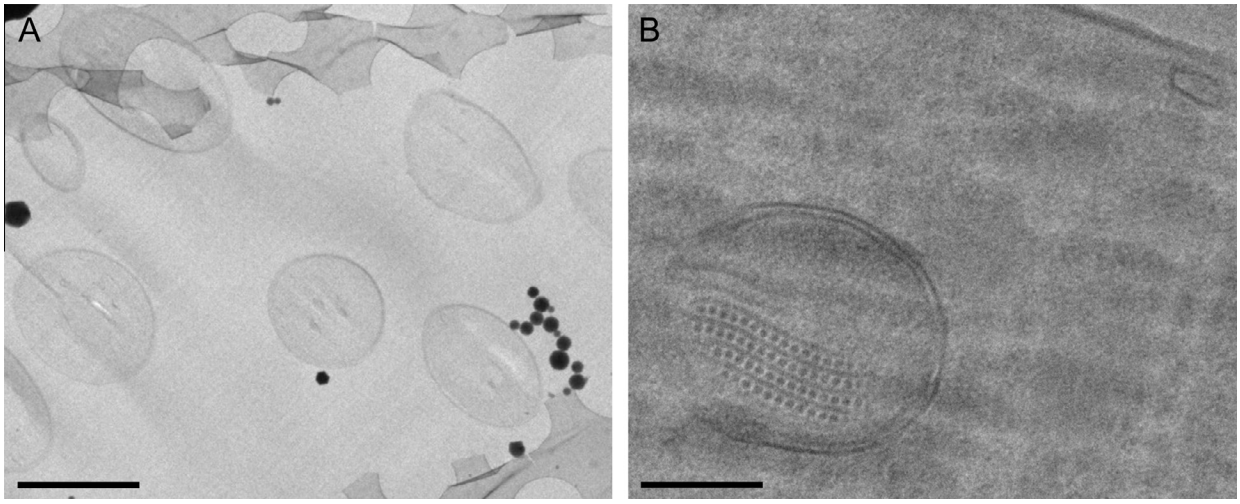

Fig.3. CEMOVIS results obtained with the new micromanipulators are shown. In (A) an overview of a yeast cell suspension is represented, with an almost undistorted cell in the center of the image. Neighboring cells are compressed from sectioning. Sections are obviously unevenly distorted. Scale bar represents 4 μm. In (B) this image shows a magnified view of the cytoplasm of a yeast cell. In the lower left corner presumably a mitochondrion with regular arrays is depicted. In the upper right corner a vesicle and a small part of the cell membrane are visible. Scale bar represents 0.1 μm.

During cryosectioning and ribbon handling, sections can get contaminated with ice particles, which are electron-opaque. Currently two approaches are available to minimize this effect. The first consists of dehumidifying the room in which the ultramicrotome is installed. However even at 20% relative humidity we found that contamination levels are often high. In the second approach, the ultramicrotome is enclosed in a Cryosphere (Leica Microsystems) in which lower relative humidity can be achieved. As an alternative, we have developed a quite efficient solution against ice contamination. It consists of a plastic cover for the cryochamber that contains openings to allow all the necessary movements for cryosectioning (Fig. 1, item 3). The reduced contact surface between warm humid air and the cryochamber significantly reduces the rate of contamination.

5. Summary

The described micromanipulators greatly facilitate the production of cryosections. The more precise control provided by the micromanipulators highly increases the yield of sections that can be observed on the electron microscope. This is especially the case for less experimented users. Sectioning artifacts still remain. However, because their severity varies within a ribbon, the larger number of sections transferred to the grid achieved with our new setup substantially increases the yield of only slightly distorted sections (Fig. 3). We anticipate that our new system will result in a more widespread application of CEMOVIS.

Acknowledgments

This work was supported by Swiss National Science Foundation Grant PP00P3_139098/1. Images were acquired on a device supported by the Microscopy Imaging Center of the University of Bern. A patent is pending. Commercialization of the described tool is foreseen.

Appendix A. Supplementary data

Supplementary data associated with this article can be found, in the online version, at http://dx.doi.org/10.1016/j.jsb.2013.11.005.

References

Al-Amoudi, A., Studer, D., Dubochet, J., 2005. Cutting artefacts and cutting process in vitreous sections for cryo-electron microscopy. J. Struct. Biol. 150, 109–121.
Al-Amoudi, A., Diez, D.C., Betts, M.J., Frangakis, A.S., 2007. The molecular architecture of cadherins in native epidermal desmosomes. Nature 450, 832–837.
Al-Amoudi, A., Castano-Diez, D., Devos, D.P., Russell, R.B., Johnson, G.T., Frangakis, A.S., 2011. The three-dimensional molecular structure of the desmosomal plaque. Proc. Natl. Acad. Sci. USA 108, 6480–6485.
Couture-Tosi, E., Ranck, J.L., Haustant, G., Pehau-Arnaudet, G., Sachse, M., 2010. CEMOVIS on a pathogen: analysis of *Bacillus anthracis* spores. Biol. Cell 102, 609–619.
Dubochet, J., Adrian, M., Chang, J.J., Homo, J.C., Lepault, J., McDowall, A.W., Schultz, P., 1988. Cryo-electron microscopy of vitrified specimens. Q. Rev. Biophys. 21, 129–228.
Eltsov, M., Maclellan, K.M., Maeshima, K., Frangakis, A.S., Dubochet, J., 2008. Analysis of cryo-electron microscopy images does not support the existence of 30-nm chromatin fibers in mitotic chromosomes in situ. Proc. Natl. Acad. Sci. USA 105, 19732–19737.
Fernandez-Moran, H., Dahl, A.O., 1952. Electron microscopy of ultrathin frozen sections of pollen grains. Science 116, 465–467.
Han, H.M., Zuber, B., Dubochet, J., 2008. Compression and crevasses in vitreous sections under different cutting conditions. J. Microsc. 230, 167–171.
Hoog, J.L., Bouchet-Marquis, C., McIntosh, J.R., Hoenger, A., Gull, K., 2012. Cryo-electron tomography and 3-D analysis of the intact flagellum in *Trypanosoma brucei*. J. Struct. Biol. 178, 189–198.
Hurbain, I., Sachse, M., 2011. The future is cold: cryo-preparation methods for transmission electron microscopy of cells. Biol. Cell 103, 405–420.
Ladinsky, M.S., Pierson, J.M., McIntosh, J.R., 2006. Vitreous cryo-sectioning of cells facilitated by a micromanipulator. J. Microsc. 224, 129–134.
Leforestier, A., Lemercier, N., Livolant, F., 2012. Contribution of cryoelectron microscopy of vitreous sections to the understanding of biological membrane structure. Proc. Natl. Acad. Sci. USA.
Matias, V.R., Al-Amoudi, A., Dubochet, J., Beveridge, T.J., 2003. Cryo-transmission electron microscopy of frozen-hydrated sections of *Escherichia coli* and *Pseudomonas aeruginosa*. J. Bacteriol. 185, 6112–6118.
Michel, M., Hillmann, T., Müller, M., 1991. Cryosectioning of plant material frozen at high pressure. J. Microsc. 163, 3–18.
Pierson, J., Fernandez, J.J., Bos, E., Amini, S., Gnaegi, H., Vos, M., Bel, B., Adolfsen, F., Carrascosa, J.L., Peters, P.J., 2010. Improving the technique of vitreous cryo-sectioning for cryo-electron tomography: electrostatic charging for section attachment and implementation of an anti-contamination glove box. J. Struct. Biol. 169, 219–225.
Pierson, J., Ziese, U., Sani, M., Peters, P.J., 2011. Exploring vitreous cryo-section-induced compression at the macromolecular level using electron cryo-tomography; 80S yeast ribosomes appear unaffected. J. Struct. Biol. 173, 345–349.
Saibil, H.R., Seybert, A., Habermann, A., Winkler, J., Eltsov, M., Perkovic, M., Castano-Diez, D., Scheffer, M.P., Haselmann, U., Chlanda, P., Lindquist, S., Tyedmers, J., Frangakis, A.S., 2012. Heritable yeast prions have a highly organized three-dimensional architecture with interfiber structures. Proc. Natl. Acad. Sci. USA 109, 14906–14911.
Salje, J., Zuber, B., Lowe, J., 2009. Electron cryomicroscopy of *E. coli* reveals filament bundles involved in plasmid DNA segregation. Science 323, 509–512.
Scheffer, M.P., Eltsov, M., Frangakis, A.S., 2011. Evidence for short-range helical order in the 30-nm chromatin fibers of erythrocyte nuclei. Proc. Natl. Acad. Sci. USA 108, 16992–16997.
Studer, D., Michel, M., Wohlwend, M., Hunziker, E.B., Buschmann, M.D., 1995. Vitrification of articular cartilage by high-pressure freezing. J. Microsc. 179 (Pt 3), 321–332.
Studer, D., Graber, W., Al-Amoudi, A., Eggli, P., 2001. A new approach for cryofixation by high-pressure freezing. J. Microsc. 203, 285–294.
Studer, D., Humbel, B.M., Chiquet, M., 2008. Electron microscopy of high pressure frozen samples: bridging the gap between cellular ultrastructure and atomic resolution. Histochem. Cell Biol. 130, 877–889.
Zuber, B., Nikonenko, I., Klauser, P., Muller, D., Dubochet, J., 2005. The mammalian central nervous synaptic cleft contains a high density of periodically organized complexes. Proc. Natl. Acad. Sci. USA 102, 19192–19197.
Zuber, B., Chami, M., Houssin, C., Dubochet, J., Griffiths, G., Daffe, M., 2008. Direct visualization of the outer membrane of *Mycobacteria* and *Corynebacteria* in their native state. J. Bacteriol. 190, 5672–5680.